Proceedings of 12th Cambridge Workshop on Cool Stars, Stellar Systems, & The Sun, 2003 University of Colorado.

The Structure and Energy Balance of the Chromosphere, Transition Region and Corona of ϵ Eri (K2 V)

C. Jordan[1], S. A. Sim[1], A. D. McMurry[2]

Abstract. Observations of ϵ Eri have been made with the Space Telescope Imaging Spectrograph (STIS) on the *Hubble Space Telescope* (*HST*). The magnetic dipole lines of Fe XII at 1242.20 and 1349.38 Å have been observed. Using lines of Si III and O IV, the mean electron pressure is 4.8×10^{15} cm^{-3} K. We discuss how comparisons between theoretical and observed emission measure distributions can be used to investigate the inhomogeneity of the corona and lower transition region. The observed line widths can be used to investigate the non-thermal heating. Evidence of two components to some line profiles is found.

1. Introduction

ϵ Eri (HD 22049, K2 V) has a shorter rotation period than the Sun ($\simeq$ 11.67 d) and larger values of parameters which indicate stellar activity. Studies of its outer atmosphere are therefore useful in understanding how the non-thermal energy requirements change with stellar activity. Here we present some results from our observations with the STIS on the *HST*. (See Jordan et al. 2001a, 2001b for stellar parameters adopted and references to earlier work.)

Although only spatially averaged values of the emission line fluxes and the electron pressure ($P_e = N_e T_e$) can be derived, we discuss methods by which information on the degree of spatial inhomogeneity can be obtained. The emission line profiles also yield information on the existence and properties of different atmospheric components.

2. Observations

Our observations with STIS include numerous lines formed in the chromosphere and transition region up to electron temperatures (T_e) of $\simeq 2.5 \times 10^5$ K. As shown in Fig. 1, we have also observed the magnetic dipole lines of Fe XII at 1242.00 Å and 1349.38 Å for the first time outside the Sun (Jordan et al. 2001a). These now allow simultaneous observations of line fluxes and widths in the upper *and* lower transition region of ϵ Eri and provide an upper limit to the electron density (N_e) at $T_e \simeq 1.4 \times 10^6$ K.

[1]Department of Physics (Theoretical Physics), University of Oxford

[2]Institute of Theoretical Astrophysics, University of Oslo

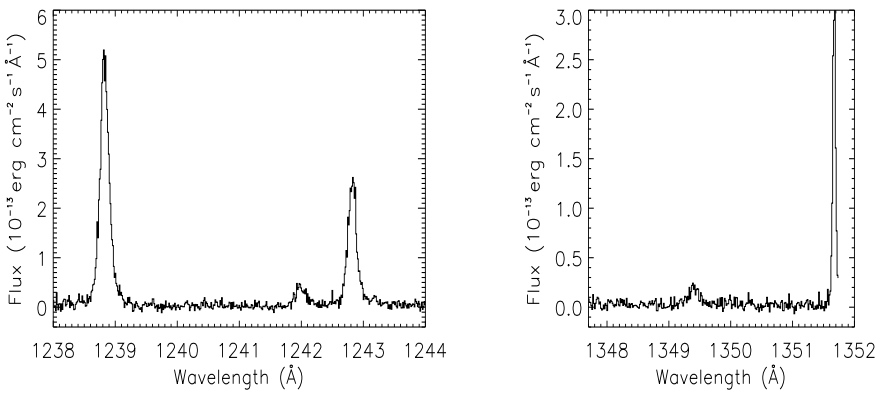

Figure 1. The spectrum of ϵ Eri showing the 1238.82- and 1242.80-Å lines of N V and the 1242.00-and 1349.38-Å lines of Fe XII.

3. Modelling

3.1. The chromosphere and lower transition region

Lines of Si III and O IV (see figs. 3 and 5 in Jordan et al. 2001b) have been used to find the mean P_e, giving $\log P_e = 15.68$. This is consistent with limits derived from lines of C III, O V and Fe XII. The mean pressure was then used to derive the emission measure loci of lines having little or no dependence on N_e. These loci correspond to the emission measures required to produce the observed line flux at each value of T_e; they are *apparent* values defined by

$$Em_{\rm app} = \int N_e N_H G(r) f(r) (A_t/A_*) {\rm d}r, \qquad (1)$$

where N_H is the hydrogen number density, G(r) is the fraction of photons not intercepted by the star, $f(r) = (r/R_*)^2$ and (A_t/A_*) is the fraction of the stellar surface area emitting the lines. Fig. 2 shows the loci and a preliminary best fit mean apparent emission measure distribution (EMD), found by iteration. Sim is re-calculating the ion fractions taking into account the density dependence of di-electronic recombination. So far this is included for the most sensitive cases of C IV, N IV and N V. Stellar photospheric abundances from Drake & Smith (1993) are used throughout.

A new model of the upper chromosphere and transition region has been derived using the mean EMD and mean P_e at 3×10^4 K, at this stage assuming a plane parallel atmosphere and $A_t/A_* = 1$. Below 6300 K the model by Thatcher et al. (1991) was adopted. The MULTI radiative transfer code was used to calculate the line fluxes and profiles. The current model reproduces the fluxes of lines formed in the upper chromosphere to within ± 50 % and transition region lines to a higher accuracy. The main differences between the new model and that of Thatcher et al. (1991) are a more gradual rise in T_e through the lower transition region and transition region electron pressures which are larger by a factor of two. The method of modelling from the mean EMD adopting hydrostatic equilibrium is described in Jordan et al. (1987).

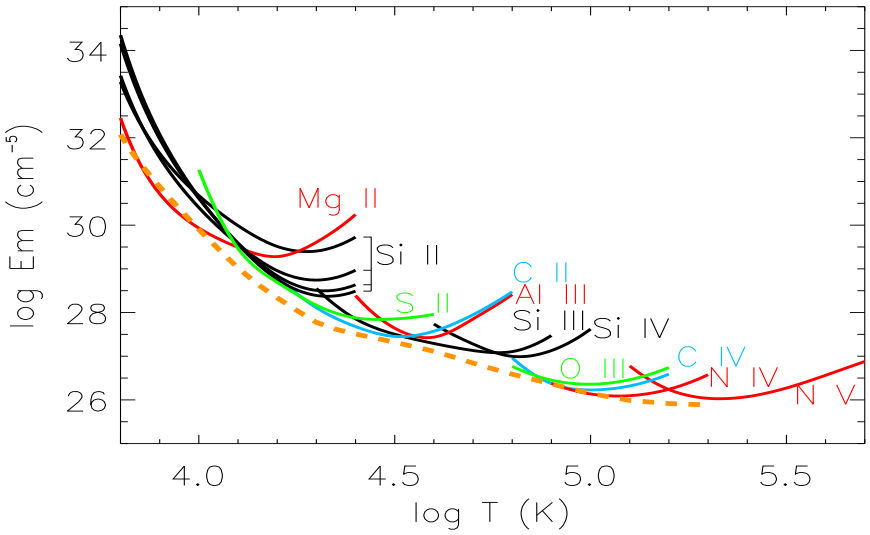

Figure 2. Emission measure loci derived from observed STIS fluxes. The dashed line is a preliminary mean apparent EMD.

3.2. The upper transition region and corona

The Fe XII 1242.00-Å line flux has been used to derive the emission measure locus around $\log T_e = 6.15$, adopting the atomic data in the CHIANTI (v3.01) data base (Landi et al. 1999). (See Fig. 3.) We have also re-analyzed the fluxes for the *EUVE* lines of iron given by Schmitt et al. (1996) using the lower hydrogen column density of $\log n_H = 17.88$ derived by Dring et al. (1997). The loci for the *EUVE* lines and their dependence on the ion populations adopted are discussed in Sim & Jordan (2001). Here we only make use of the coronal temperature, T_c, that corresponds to the maximum value of the EMD.

In spatially integrated observations, the observed flux in collisionally excited coronal emission lines comes predominantly from the first pressure-squared scale height, well below the height where the main heating occurs. We assume that above $T_e = 2 \times 10^5$ K the heating by the net conductive flux from the overlying corona is balanced by the local radiation loss. The true emission measure for a plane parallel atmosphere (to simplify the presentation) is defined by

$$Em_t(0.3) = \int_{\Delta h} N_e N_H dh \simeq \frac{0.83 P_e^2}{\sqrt{2} T_e} \frac{\mathrm{d}h}{\mathrm{d}T_e}, \tag{2}$$

where Δh corresponds to $\Delta \log T_e = 0.3$.

Using the conductive flux equation

$$F_c = -\kappa T_e^{5/2} \mathrm{d}T_e/\mathrm{d}h, \tag{3}$$

(where $\kappa T_e^{5/2}$ is the coefficient of thermal conduction), to substitute for $\mathrm{d}h/\mathrm{d}T_e$ in equation (2), and using the assumed energy balance (with a variable A_t),

allows the emission measure distribution to be calculated from starting values of T_c, P_c and $Em(T_c)$ (see Jordan 1996). I.e.

$$\frac{\mathrm{d}\log Em_t(0.3)}{\mathrm{d}\log T_e} = \frac{3}{2} + 2\frac{\mathrm{d}\log P_e}{\mathrm{d}\log T_e} + \frac{\mathrm{d}\log A_t}{\mathrm{d}\log T_e} - \frac{2P_{\mathrm{rad}}(T_e)Em_t(0.3)^2}{0.83\kappa P_e^2 T_e^{3/2}}, \qquad (4)$$

where $P_{\mathrm{rad}}(T_e)$ is the radiative powerloss function.

Fig. 3 (thin solid line) shows the locus derived from the Fe XII 1242-Å line flux and the EMD (dashed line) which reproduces this flux using $\log T_c = 6.4$ (from the *EUVE* observations) and a pressure of $\log P_e = 15.80$, from the Fe XII lines. Here we assume that A_t is constant. For a given value of P_e and T_c there is a *maximum* value of $Em(T_c)$ that will satisfy the energy balance equation. This value can be found by increasing $Em(T_c)$ until no solution is possible. The *observed* emission measure is the spatially averaged value given by

$$Em_t(0.3)A_t = Em_{\mathrm{av}}(0.3)A_*. \qquad (5)$$

Any difference between Em_{av} and the maximum calculated value of Em_t can be attributed to the term $f_c = A_t/A_*$; thus comparing Em_{av} with $Em_t(\mathrm{max})$ allows the *lower limit* on f_c to be derived. For ϵ Eri the value of $Em_t(\mathrm{max})$ is close to that observed, leading to $f_c \simeq 1.0$. The electron pressure used can also be varied. With $\log P_e = 15.60$, the maximum emission measure (dotted line in Fig. 3) fails to reproduce the observed Fe XII flux. With $\log P_e = 16.00$ the upper limit to the emission measure (thick solid line in Fig. 3) leads to $f_c \geq 0.6$. Thus taking $\log P_e = 15.80 \pm 0.20$ gives $f_c \geq 0.6$.

The best fit EMD (dashed line in Fig. 3) at $\log T_e = 5.30$ is an order of magnitude greater than Em_{av} derived from the STIS lines. The calculated *true* emission measure at $\log T_e = 5.3$ can be reconciled with Em_{av} if the transition region emission at this T_e originates predominantly from only 10% of the area. An alternative way of showing this is to use the existence of the minimum in the EMD (see eq. 4), and the measured P_e, to derive the true emission measure at $\log T_e = 5.30$ (see Jordan 1996).

The fractional areas derived *increase* if a higher value of $\log T_c$ is adopted, but the pressure required is then larger than the limit implied from the Fe XII line fluxes. The fractional areas *decrease* if an abundance of iron lower than the stellar photospheric value is adopted (see Sim & Jordan 2001 for details).

4. Line Widths

The observed widths (corrected for the small instrumental broadening), of lines which are estimated to be optically thin, have been derived using single Gaussian fits. These have been used to obtain the non-thermal widths (ξ) as a function of T_e, as shown in Fig. 4. Values of ξ are shown at $\log T_e \pm 0.10$, where T_e is the calculated optimum temperature for the line formation. The variation of ξ with T_e is broadly similar to that found for the Sun (see e.g. Chae et al. 1998) but in ϵ Eri, ξ appears to decrease or flatten off by $\log T_e \simeq 5.1$.

The values of ξ are slightly *smaller* than the solar values. If ξ is associated with an upward propagating Alfvén wave flux, then energy dissipation is implied

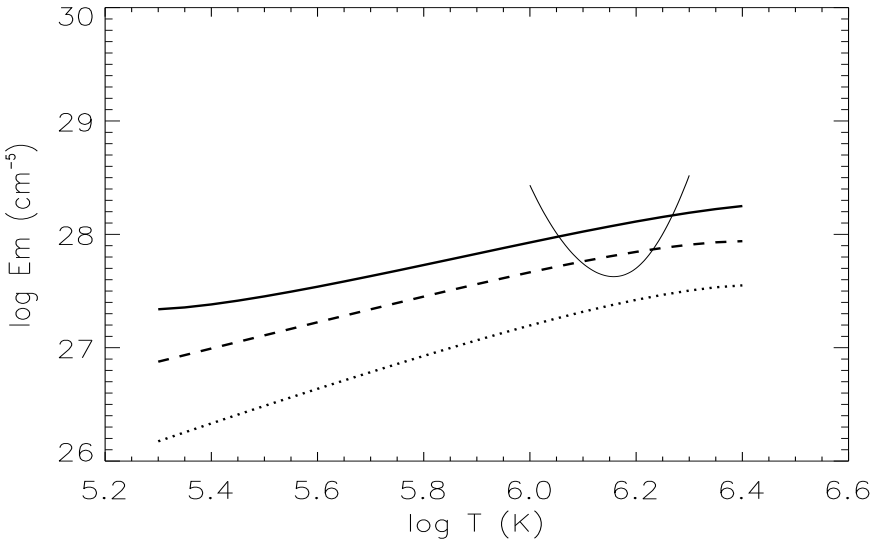

Figure 3. Emission measure locus derived from the Fe XII 1242.00-Å line flux (thin solid line); the EMD reproducing this flux using $\log T_c = 6.4$ and $\log P_e = 15.8$ (dashed line); maximum emission measures found using $\log P_e = 16.0$ and 15.6 (thick solid and dotted lines.

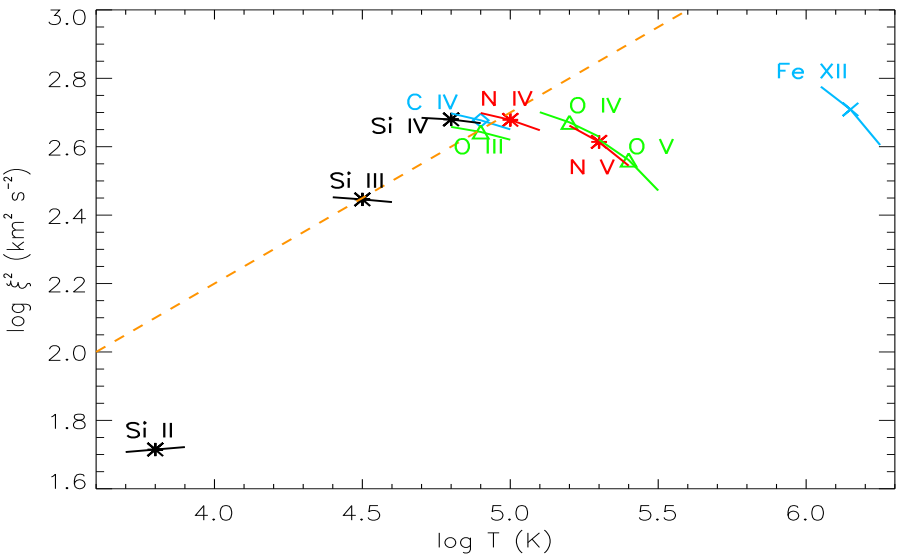

Figure 4. Non-thermal line widths (ξ) derived from single Gaussian fits to the profiles observed with STIS.

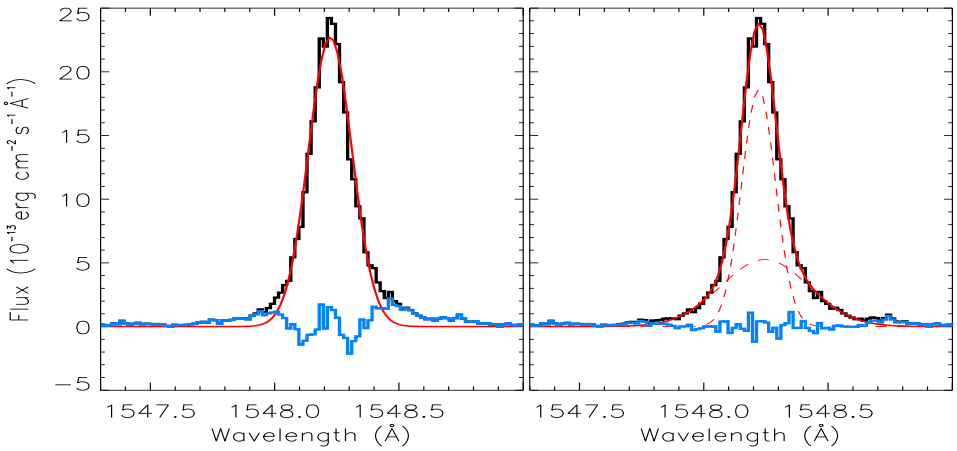

Figure 5. Single (left panel) and two-Gaussian (right panel) fits to the observed C IV 1548.20-Å line profile. The observed profile is shown in black; fits are shown in red and residuals are shown in blue.

when the gradient of ξ^2 versus T_e is < 0.5. A gradient of 0.5, fitted to the Si III width is shown; this will not apply below $\log T_e \simeq 4.2$, where the mean molecular weight is not constant. Since the upper transition requires very little heating above $\log T_e = 5.3$, this hypothesis is apparently not consistent with the observations. However, the mean geometry of the magnetic field between the low transition region and the corona also needs to be taken into account.

Also, some of the observed line widths are not fitted exactly by a single Gaussian profile – as found in the Sun (e.g. by Peter 2000a,b) and in other stars (e.g. by Woods et al. 1997). Fig. 5 shows the C IV line at 1548.20 Å, fitted with a single Gaussian (left hand panel) and with narrow and broad components (right hand panel). The residuals are shown in each case. The narrow core is *not* redshifted to within the accuracy of the measurements ($\simeq 4$ km s^{-1}), but the broad component shows a slight redshift (see also Jordan et al. 2001a). The fits to other line profiles and the variation of the widths of both components with T_e will be discussed in a forthcoming paper.

5. Energy Requirements

The spatially averaged radiative losses can be found from

$$\Delta F_{\rm rad} A_t = Em_{\rm av}(0.3) P_{\rm rad}(T_e) A_* = Em_t(0.3) P_{\rm rad}(T_e) A_t \qquad (6)$$

Ignoring the area factors the total radiative flux between 2×10^4 K and 2×10^5 K is $\simeq 1.5 \times 10^6$ erg cm^{-2} s^{-1}, while F_c at 2×10^5 K is an order of magnitude larger, and has the wrong dependence on T_e to account for the form of the EMD below 2×10^5 K. However, with the area factor of 10%, the true EMD and radiative losses are a factor of 10 larger, while the conductive flux is reduced by a factor of 10. An additional heating source is then required below 10^5 K.

The energy carried down by thermal conduction at $T_e = 1.4 \times 10^6$ K, where the Fe XII lines are formed, is $\simeq 6.6 \times 10^6$ erg cm^{-2} s^{-1}. Using the observed value of ξ and $\log P_e = 15.80$, the energy carried by Alfvén waves would be $\simeq 2 \times 10^5 B$ erg cm^{-2} s^{-1}, where B is the magnetic flux density. For these values of the flux to agree (ignoring the smaller radiation losses) requires $B = 33$ G. Since the spatially averaged surface field is 165 G (Rüedi et al. 1997), not all the surface magnetic flux need extend to the corona.

6. Conclusions

The new observations with STIS have allowed both the upper and lower transition regions of ϵ Eri to be investigated through emission lines fluxes and line widths. The average value of P_e is about an order of magnitude larger than the equivalent average solar value. The corona appears to have an area filling factor of unity, but by considering the likely energy balance we deduce that the emission from the lower transition region comes predominantly from around 10% of the area. Models with a varying emitting area are now required. Two component models also need to be investigated, given the presence of (at least) two components to the line widths.

References

Chae, J., Schühle, U. & Lemaire, P. 1998, ApJ, 505, 957

Drake, J.J., Smith, G. 1993, ApJ, 412, 797

Dring, A.R., Linsky, J.L., Murthy, J., Henry, R.C., Moos, W., Vidal- Madjar, A., Audouze, J. & Landsman, W. 1997, ApJ, 488, 760

Jordan, C. 1996, Ap&SS, 237, 134

Jordan, C., Ayres, T.R., Brown, A., Linsky, J.L. & Simon, T. 1987, MNRAS, 225, 903

Jordan, C., McMurry, A.D., Sim, S.A. & Aruvel, M. 2001a, MNRAS, 322, L5

Jordan, C., Sim, S.A., McMurry, A.D. & Aruvel, M. 2001b, MNRAS, 326, 303

Landi, E., Landini, M., Dere, K.P., Young, P.R. & Mason, H.E. 1999, A&AS, 135, 339

Peter, H. 2000a, A&A, 360, 761

Peter, H. 2000b, A&A, 364, 933

Rüedi, L., Solanki, S.K., Mathys, G. & Saar, S.H. 1997, A&A, 318, 429

Schmitt, J.H.M.M., Drake, J.J., Stern, R.A. & Haisch, B.M. 1996, ApJ, 457, 882

Sim, S.A. & Jordan, C. 2001, in *Stellar Coronae in the CHANDRA and XMM-NEWTON Era*, 35th ESLAB Symposium, ESA, Nordwijk, 231

Thatcher, J.D., Robinson, R.D., & Rees, D.E. 1991, MNRAS, 250, 14

Wood, B.E., Linsky, J.L. & Ayres, T.R. 1997, ApJ, 478, 745